

# Studying the Mechanical and Thermal Properties of Polymer Nanocomposites Reinforced with Montmorillonite Nanoparticles Using Micromechanics Method

M.H. Yas <sup>1,\*</sup>, H. Shahrani Korani <sup>1</sup>, F. Zare Jouneghani <sup>2</sup>

<sup>1</sup>Department of Mechanical Engineering, Razi University, Kermanshah, Iran

<sup>2</sup>Young Researchers and Elite Club, Shahrekord Branch, Islamic Azad University, Shahrekord, Iran

Received 28 September 2019; accepted 14 December 2019

## ABSTRACT

In this study, the mechanical and thermal behavior of the nano-reinforced polymer composite reinforced by Montmorillonite (MMT) nanoparticles is investigated. Due to low cost of computations, the 3D representative volume elements (RVE) method is utilized using ABAQUS finite element commercial software. Low-density poly ethylene (LDPE) and MMT are used as matrix and nanoparticle material, respectively. By using various geometric shapes and weight fractions of nanoparticle, the mechanical and thermal properties such as Young's modulus, shear modulus, heat expansion coefficient and heat transfer coefficient are studied. Due to addressing the properties of interfacial zone between the matrix and nanoparticle, finite element modeling is conducted in two ways, namely, perfect bonding and cohesive zone. The results are validated by comparing with experimental results reported in literature and a reasonable agreement was observed. The prediction function for Young's modulus is presented by employing Genetic Algorithm (GA) method. In addition, Kerner and Paul approaches as theoretical models are used to calculate the Young's modulus. It was finally concluded that the magnitude of the Young's and shear modules increase by adding MMT nanoparticles. Furthermore, increment of MMT nanoparticles to polymer matrix nanocomposite decrease the heat expansion and heat transfer coefficients.

© 2020 IAU, Arak Branch. All rights reserved.

**Keywords:** Polymer nanocomposite; Montmorillonite (MMT); Finite element method (FEM); Representative volume elements (RVE).

## 1 INTRODUCTION

**I**NHERENT behaviors of the pristine polymer are not sufficient and are needed to be modified by mixing with appropriate materials. For instances, we can consider combining elastomers such as ethylene-propylene-diene monomer and high density poly ethylene or blending of nylon-6 and clay nanoparticles to enhance the intrinsic properties of pristine polymer. Many researchers have widely dedicated their researches to this subject so far. For

\*Corresponding author.

E-mail address: yas@razi.ac.ir (M.H.Yas).

example, Fornes et al. [1] examined the reinforcement of nylon 6 by layered aluminosilicates (LAS) and glass fibers by utilizing Halpin–Tsai and Mori–Tanaka as composite theories. Karamane et al. [2] prepared methacrylate/clay nanocomposite via in-situ polymerization. Their results illustrate that the increase in clay loading leads to a slight decrease in the mechanical properties. Mahmood et al. [3] presented MMT clay encapsulation in polyethylene glycol (PEG) by an electro spraying process. Paliwal et al. [4] suggested the nano-mechanical modeling of interfaces of polyvinyl alcohol (PVA)/clay nanocomposite. The results showed that PVA/clay nanocomposites with higher degree of exfoliation compared with nanocomposites with higher clay-intercalation have higher strength under tensile loading. Zeng et al. [5] proposed simulation of polymer nanocomposites. They presented some computational procedures that have been applied to nanocomposites to understand and predict capability of polymer nanocomposites. Moreover, they founded that molecular simulation is useful to investigate molecular interactions and structures in the scale of nanometer. Zeng et al. [6] investigated clay-based polymer nanocomposites and showed that clay nanoparticles, owing to their specific layered structure and availability at low cost, are promising nanoparticle reinforcements for polymers to fabricate low cost, light-weight and high performance nanocomposites. Raja et al. [7] studied influence of three-dimensional nanoparticle branching on the Young's modulus of nanocomposites and they illustrate that branched nanofillers have the potential for optimization of Young's modulus over their linear counterparts. Wang et al. [8] developed numerical simulation to investigate the effect of interfacial bonding on interphase properties in SiO<sub>2</sub>/Epoxy nanocomposite. Plethora of studies has been done to recognize the behavior of reinforced nanocomposites by using approaches such as molecular dynamic (MD) simulations [9-13], analytical [1, 14, 15], computational continuum based theories [16], and multi scale methods [17-20]. To assess the elastic properties of nanocomposites, a feasible method is to build up a representative volume element (RVE) included by a cubic body of matrix with a nanoparticle. In the theory of composite materials, the representative elementary volume (REV) or the RVE or the unit cell is the smallest volume over which a measurement can be made that will yield a value representative of the whole [21]. Shahzamanian et al. [22] evaluated the effective elastic properties of Cementitious materials by using RVE method. Ali et al. [23] used the RVE model to analyze the effect of Boron Nitride nanotubes in Beta Tricalcium Phosphate and Hydroxyapatite elastic modulus. Based on the asymptotic homogenization method, a description of the derivation of the local problems and the formulae to obtain all homogenized effective coefficients of a thermomagneto-electroelastic (TMEE) periodic heterogeneous media were given [24]. Lezgy-Nazargah et.al developed a fully micromechanical model for estimating the effective coupled thermo-electro-elastic material coefficients of three-phase piezoelectric structural fiber composites [25]. Lezgy-Nazargah developed a fully micromechanical model based on iso-field assumptions for computing the effective coupled thermo-electro-elastic material properties of Macro Fiber Composites (MFCs) in the linear regime [26].

Novel to this work is to investigate the role of MMT clay nanoparticle in the mechanical and thermal behavior of polymer matrix nanocomposite. Also, we develop representative volume element (RVE) model that pave the way for nanocomposite simulations to study nanocomposites conveniently. Numerical results are compared with the studies reported in the literatures. The rest of the article is organized as follows. In section 2, the finite element procedure such as material model, boundary conditions, and so on are described. In section 3, numerical results and discussion about results are considered, and finally in section 4, some main conclusions are presented.

## 2 NUMERICAL SIMULATION

In order to study the effects of nanoparticle, which used to strength the nano-reinforced polymer composite on the mechanical and thermal properties, the simulation was done by ABAQUS 6.14 considering general static and 3D analysis.

### 2.1 Finite element method

Owing to declining computational cost, all of the numerical simulations were performed with a three dimensional RVE model as indicated in Fig.1. The selected sector dimensions are,  $D = 50mm$  with three different values of  $L$ . The finite element solution converged for the element size of 3 nm with type of C3D8R, which has an 8-nodes linear element. The mesh gridding is shown in Fig. 2.

One of the most important subjects in such simulations is how to model interaction surface between the polymer matrix and the nanoparticle. Perfect bounding (tie constraint) and cohesive zone model method are two common

methods for simulating this procedure. In this work, the two types of constraint are used and results are compared with each other.

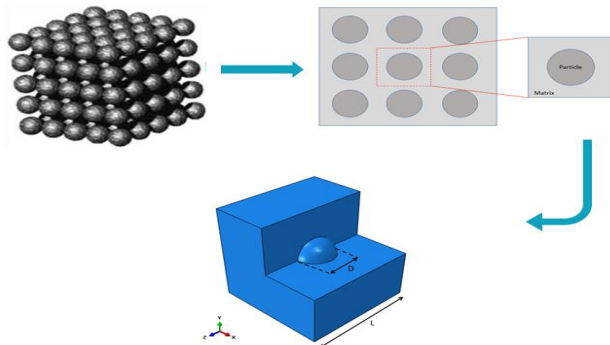


**Fig.1**  
The RVE geometry and assembly model used in the simulation.

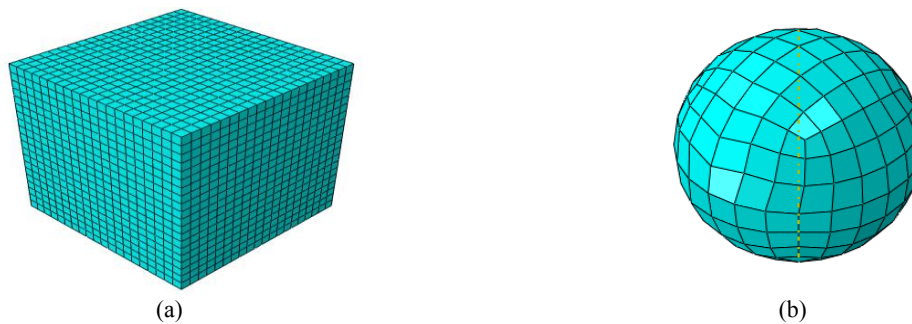


**Fig.2**  
RVE's mesh (a) polymer matrix nanocomposite (b) MMT nanoparticle.

## 2.2 Material property

In this study, the linear low-density polyethylene with trade name LL209AA and MMT are used as the polymer matrix and nanoparticle, respectively. These materials are widely used in industry particularly in automotive field due to their low density compared to metals and their specific advantages over the plastics [27]. The mechanical and thermal properties of materials are provided in Table 1.

**Table 1**  
Mechanical and thermal properties of MMT and LDPE.

Material	$E$ (GPa)	$\nu$	$\rho$ ( $gr/cm^3$ )	$\alpha$ ( $10^{-5}/^{\circ}C$ )	$K$ (W / m.K)
Montmorillonite	178	0.2	2.83	0.59	0.15
LDPE	0.105338	0.35	0.92	24	0.33

## 2.3 Model validation

In order to verify the accuracy of numerical results in the finite element simulation, the Young's modulus against weight fraction of MMT nanoparticles was compared with the experimental one reported by Yas et al. [28] as shown in Fig. 3.

As observed in Fig. 3 the comparison shows pretty a reasonable agreement between the empirical and the present results, which provides some verification of the simulation model. It should be noticed that the difference between experimental and numerical results might be attributed to the some errors that may be happened in the experimental test conditions or probably due to some technical issues during preparation of the nanocomposite, which were not considered in the RVE model.

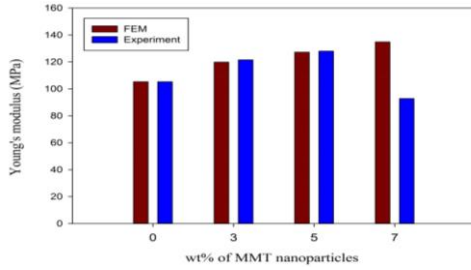


**Fig.3**  
Comparison between experimental and numerical results.

### 3 NUMERICAL RESULTS AND DISCUSSION

In the current work, the numerical simulations of the polymer matrix nanocomposite reinforced with MMT nanoparticle under tensile loading test were performed. The simulations are examined for deriving mechanical and thermal properties of nano-reinforced polymer composite based on two different models. The first model is obtained by applying tie constraint (Perfect bounding) and the second one is based on the cohesive zone model. It is noteworthy that all the mechanical results are obtained along the surface, which is created by opting elements in the middle of the cubic model as illustrated in Fig. 4.

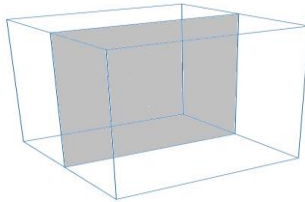


**Fig.4**  
Element sets of nanocomposite.

#### 3.1 The effect of weight fraction on the Young's and shear modulus

The general stress-strain relations are used to calculate the Young's modulus as expressed in Eq. (1) [29].

$$\begin{pmatrix} \varepsilon_x \\ \varepsilon_y \\ \varepsilon_z \end{pmatrix} = \begin{bmatrix} \frac{1}{E} & -\frac{\nu}{E} & -\frac{\nu}{E} \\ -\frac{\nu}{E} & \frac{1}{E} & -\frac{\nu}{E} \\ -\frac{\nu}{E} & -\frac{\nu}{E} & \frac{1}{E} \end{bmatrix} \begin{bmatrix} \sigma_x \\ \sigma_y \\ \sigma_z \end{bmatrix} \tag{1}$$

where,  $\varepsilon_x$ ,  $\varepsilon_y$ , and  $\varepsilon_z$  are strains along  $x$ ,  $y$ , and  $z$  directions, respectively.  $\sigma_x$ ,  $\sigma_y$  and  $\sigma_z$  are stresses in  $x$ ,  $y$ , and  $z$  directions, respectively. Also,  $E$  and  $\nu$  are Young's modulus and Poisson's ratio, respectively. Since the finite element model is symmetric, the above equations are reduced to one equation in the direction of tensile load. As observed in Fig. 5, RVE is subjected to tensile loading in  $x$  direction.

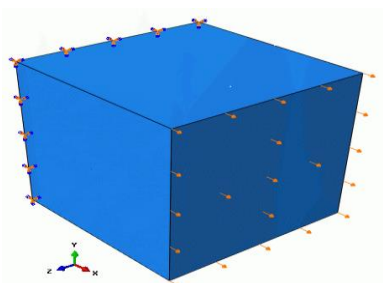


**Fig.5**  
Tensile loading direction.

In tensile loading, strain component in transverse plane can be defined as Eq. (2):

$$\varepsilon_x = \frac{\Delta L}{L} \quad (2)$$

where,  $\Delta L$  is change in length of RVE and  $L$  referees to initial length. By integrating and calculating the average of stress and strain in  $Z$ - $Y$  plane which is indicated in Fig.4, the mean stress and strain can be calculated as:

$$\sigma_{ave} = \frac{1}{A} \int_A \sigma_x(0, y, z) dydz \quad (3)$$

$$\varepsilon_{ave} = \frac{1}{A} \int_A \varepsilon_x(0, y, z) dydz \quad (4)$$

where,  $A$  is the area of the RVE's middle surface section. The Young's modulus can be obtained by dividing Eq.(3) to Eq.(4) as:

$$E_x = \frac{\sigma_{ave}}{\varepsilon_{ave}} \quad (5)$$

Three different weight fractions of 3, 5, and 7% for two types of entire bounding including tie constraint and cohesive zone model were studied in this paper. The corresponding bar charts are shown in Fig.6 and Fig.7.

Fig.6 and Fig.7 clearly show that increase in weight fraction of MMT nanoparticle results in the increase of the Young's modulus of nano-reinforced polymer composite. Based on the definition of the shear modulus, there is straight relationship between the shear modulus and the Young's modulus, it can be concluded that by increasing the weight fraction of MMT nanoparticle, the shear modulus of nano-reinforced polymer composite increases.

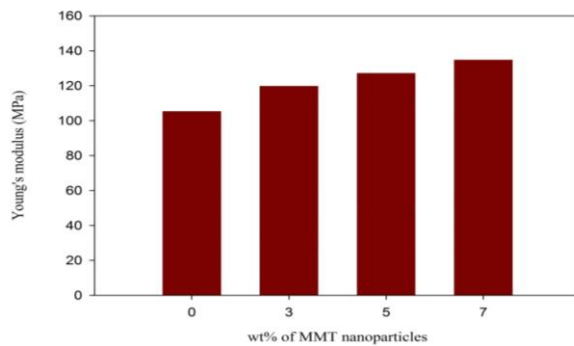


**Fig.6**  
The effect of weight fractions on the Young's modulus with perfect bounding.

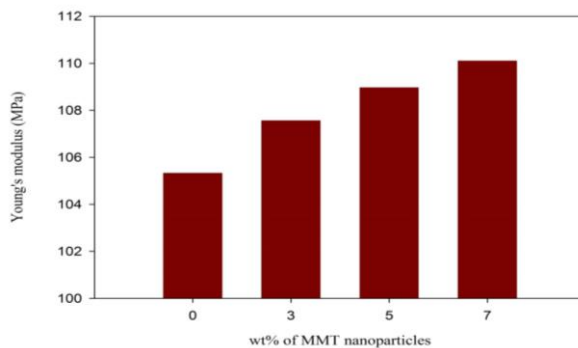


**Fig.7**  
The effect of weight fractions on the Young's modulus with cohesive zone model.

### 3.2 The effect of nanoparticle diameter on the Young's modulus

The properties of the polymer matrix are strengthened by adding nanoparticle because nanoparticles have extremely active surface as well as high surface to volume ratio. The surface to volume ratio for particles can be stated as:

$$\frac{A_{particle}}{V_{particle}} = \frac{4\pi r^2}{4/3\pi r^3} = \frac{3}{r} \quad (6)$$

Three diameters of 20, 40, and 50 nm were considered in this study. The Young's modulus for each diameter of two cases of perfect bounding and cohesive zone model are shown in Fig.8 and Fig.9, respectively.

The results shown in Fig.8 and Fig.9 clearly indicate that the Young's modulus decreases with the increase in diameter of nanoparticle. For instance, for the diameter of 25 nm, the Young's modulus is approximately 119.75 and 107, for two different models respectively. It is prognosticated that the value of the Young's modulus derived in case of cohesive zone model is slightly lower than which one in case of perfect bounding.

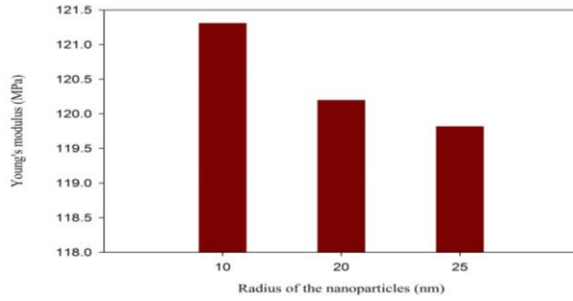


**Fig.8**  
The effect of nanoparticle radiuses on the Young's modulus with perfect bounding.

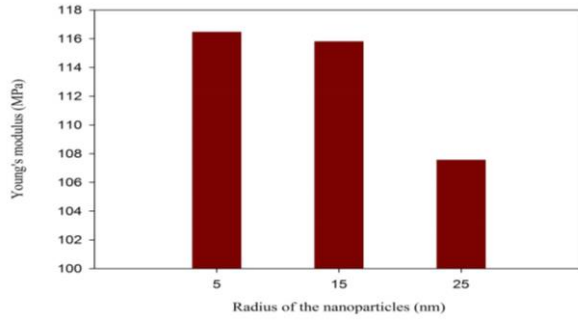


**Fig.9**  
The effect of nanoparticle radiuses on the Young's modulus with cohesive zone model.

### 3.3 The effect of weight fraction on heat expansion coefficient

In order to calculate the heat expansion coefficient, the general equation of stress-strain relation under mechanical and thermal loading expressed as follows:

$$\begin{pmatrix} \varepsilon_x \\ \varepsilon_y \\ \varepsilon_z \end{pmatrix} = \begin{bmatrix} \frac{1}{E} & -\frac{\nu}{E} & -\frac{\nu}{E} \\ -\frac{\nu}{E} & \frac{1}{E} & -\frac{\nu}{E} \\ -\frac{\nu}{E} & -\frac{\nu}{E} & \frac{1}{E} \end{bmatrix} \begin{bmatrix} \sigma_x \\ \sigma_y \\ \sigma_z \end{bmatrix} + \alpha \Delta T \begin{bmatrix} 1 \\ 1 \\ 1 \end{bmatrix} \quad (7)$$

Indeed,  $\alpha$  is heat expansion coefficient and  $\Delta T$  is change in temperature. Due to lack of mechanical loading in x, y and z directions and symmetric geometry of RVE, Eq. (7) is reduced as follows:

$$\varepsilon_x = \alpha \Delta T \quad (8)$$

Three weight fractions including 3, 5, and 7% were considered to investigate the effect of weight fraction on the heat expansion coefficient. The heat expansion coefficient against various weight fractions is shown in Fig.10.

Fig.10 clearly illustrates that increase in the weight fraction of the MMT nanoparticle results in decrease of the heat expansion coefficient.

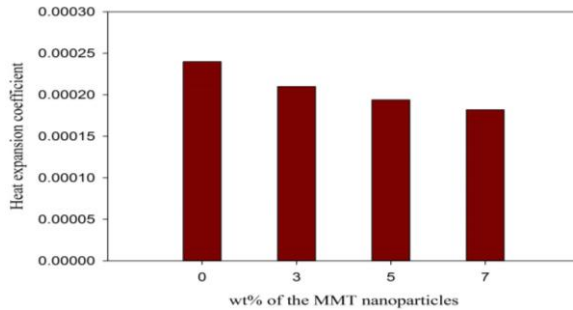


**Fig.10**  
Variations of the heat expansion coefficient versus different weight fractions of nanoparticle.

### 3.4 The effect of weight fraction on heat conductivity coefficient

In order to derive the heat conductivity coefficient, the simulation was done under heat flux boundary conditions. To do this, the heat flux was applied to nano-reinforced polymer composite as shown in Fig.11.

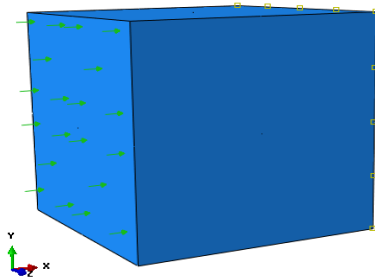
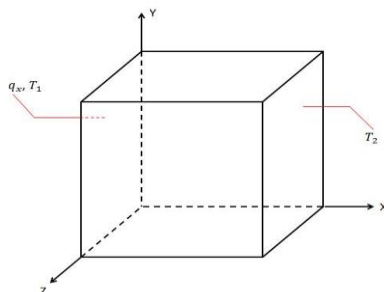


**Fig.11**  
Surface heat flux boundary conditions.

In this case, simulations were done with three different weight fractions of 3, 5, and 7%. It should be noted that the heat conductivity ( $K_{eff}$ ) and heat transfer relation ( $q_x$ ) relations can be defined as follows:

$$K_{eff} = -\frac{q_x L}{\Delta T} \quad (9)$$

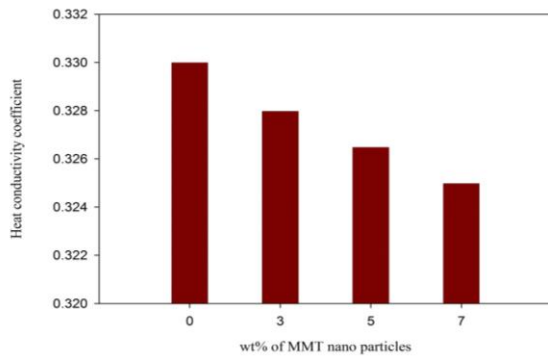
where,  $q_x$  and  $\Delta T = T_2 - T_1$  are assumed according to Fig.12.  $T_2$  and  $q_x$  are defined as boundary conditions and  $T_1$  is derived from simulation.



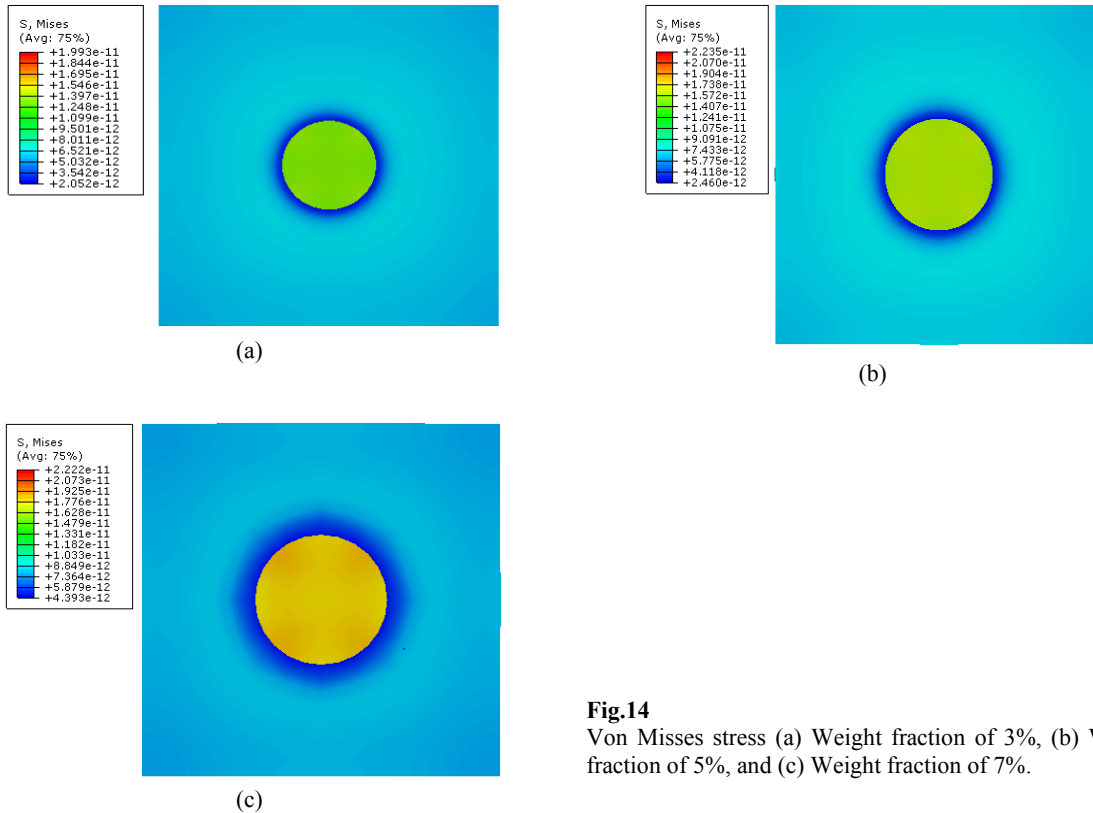
**Fig.12**  
Boundary conditions.

Fig.13 depicts the heat conductivity for different values of the weight fractions of MMT nanoparticle. Fig.13 indicates that the heat transfer coefficient is pretty decreased with the increase of the weight fractions of MMT nanoparticle. The results shown in Figs. 6, 7, 8, 9, 10, and 13 clearly indicate that how it is possible to modify mechanical and thermal properties of nano-reinforced polymer composites by adding nanoparticles. As the results illustrated in Figs. 6 and 7 suggest, the increase in percentage of weight fraction results an ascending trend in the Young's modulus in two various types of interfacial zone modeling. Analogous trend can be seen for the shear modulus versus percentage of nanoparticle's weight fraction. Moreover, Based on Figs. 8, 9, in perfect bounding and cohesive zone modeling, the increase in the radius of the nanoparticle follows a diminishing trend in the Young's modulus. Furthermore, Figs. 10 and 13 apparently show that heat expansion and heat conductivity coefficients decrease by increasing in percentage of the nanoparticle weight fraction. It is noteworthy that the Young's modulus in case of perfect bounding model is always over the Young's modulus in case of cohesive zone modeling for various values of nanoparticle's weight fraction percent. In order to investigate the distribution of von Misses stress for nanocomposite with presence of clay nanoparticle, von Misses stress counter is shown in Fig.14 with various weight fractions of MMT nanoparticle in case of perfect bounding model.

As shown in Fig. 14, a large amount of von Misses stress is carried by MMT nanoparticle with respect to matrix.



**Fig.13**  
Variations of heat conductivity coefficient versus different weight fractions of nanoparticle.



**Fig.14**  
Von Misses stress (a) Weight fraction of 3%, (b) Weight fraction of 5%, and (c) Weight fraction of 7%.

### 3.5 Theoretical prediction by genetic algorithm

In this paper, in order to predict the mechanical and thermal properties for any weight fraction without considering agglomeration of nanoparticle, Genetic Algorithm (GA) is implemented in a Matlab code. GA procedure is a strong tool to find an accurate solution to a complex optimization issues [30]. First, it is assumed the material properties can be described by a simple polynomial depending on the nanoclay weight percentage. The coefficients of this polynomial function are found by maximizing the accuracy. The “ $1 - R_{adj}^2$ ” is introduced as fitness function which is to be minimized. “ $R_{adj}^2$ ” is accuracy criterion of an arbitrary mechanical property function (such as Young’s modulus). “ $R_{adj}^2$ ” is defined as a process which is demonstrated below. The mechanical property is function of nanoclay weight percent and “ $R_{adj}^2$ ” is a function of coefficients which are introduced below.  $M_i$  and  $W$  are considered as the mechanical properties and the nano clay weight percent respectively. The  $M_i$  is expressed as a polynomial function of  $W$  as follows:

$$M_i = \sum_{j=0}^4 a_{ji} W^j \quad (10)$$

Now, the coefficients  $a_{ji}$  are found by maximizing the accuracy of polynomial function. The equations can be written as:

$$R_{adj}^2 = 1 - \frac{VAR_E}{VAR_T} \quad (11)$$

In which

$$VAR_E = SS_{Err} / (n - k - 1) \quad (12)$$

$$VAR_T = SS_{Tot} / (n - 1) \quad (13)$$

$$SS_{Tot} = \sum_{i=1}^n (y_i - \bar{y})^2 \quad (14)$$

$$SS_{Err} = \sum_{i=1}^n (y_i - M_i)^2 \quad (15)$$

$$\bar{y} = \frac{1}{n} \sum_{i=1}^n y_i \quad (16)$$

$$M_i(W) = a_{0i} + a_{1i}W + a_{2i}W^2 + a_{3i}W^3 \quad (17)$$

In these equations  $n=4$  is the number of experiments,  $k=0$  is the number of duplicated experiments and  $y_i$  denotes the experimentally measured mechanical properties.  $a_{ji}$  coefficients are obtained after approximately 40 generations by minimization of “ $1 - R_{adj}^2$ ” through using MATLAB. Obtaining the  $a_{ji}$ , coefficients, the mechanical and thermal properties modulus of uniformed distribution can be expressed as function of nanoclay weight percent as follows:

$$E(Wt) = 10^6 [0.0355Wt^3 - 0.5086Wt^2 + 6.0332Wt + 105.34] \quad (18)$$

$$E(Wt) = 10^6 [0.0923Wt^3 - 0.9665Wt^2 + 4.485Wt + 101.73] \quad (19)$$

$$\alpha(Wt) = 10^{-5} [0.0014Wt^3 + 0.0286Wt^2 - 1.0986Wt + 24] \quad (20)$$

$$K(Wt) = 2 \times 10^{-6}Wt^3 - 3 \times 10^{-5}Wt^2 - 0.0006Wt + 0.33 \quad (21)$$

where,  $Wt$  is MMT clay nanoparticle weight fraction.

In order to verify mechanical properties such as the elastic modulus, the present results for Young's modulus based on Eqs. (18,19) are compared to theoretical models proposed by Kerner [31, 32] and Paul [32, 33]. Kerner and Paul prediction in case of perfect interfacial adhesion can be stated as follows, respectively:

$$\frac{E_c}{E_m} = 1 + 11.6\varphi - 44.4\varphi^2 + 96.3\varphi^3 \quad (22)$$

$$\frac{E_c}{E_m} = \frac{1 + (m-1)\varphi^{2/3}}{1 + (m-1)(\varphi^{2/3} - \varphi)} \quad (23)$$

where subscripts of  $c$  and  $m$  are referring to composite and matrix, respectively. Moreover,  $m$  is ratio of nanoparticle's elastic module and the elastic modulus of matrix and  $\varphi$  is volume fraction of nanoparticle, which can be defined as correction form of bellow:

$$\varphi = \frac{Wt}{D_p^{1/3}} \quad (24)$$

Table 2., shows ratio values of  $\frac{E_c}{E_m}$  based on Kerner and Paul theories which are compared to experimental ones presented by Yas et al. [28] as well as the present numerical results.

Based on the results provided in Table 2. , it is clear that the values of Young's module in case of experiment and FE are tiny smaller than those calculated using the Kerner and Paul prediction models. This deviation mainly is due to neglecting agglomerating effects. Former studies showed that when the agglomerates of nanoparticles are considered in polymer matrix, the predicted elastic modulus decreases [32]. Furthermore, according to mechanical behavior results derived in two various types of interfacial zone, namely perfect bounding and cohesive zone modeling, it is well-known that mechanical behavior of composites can be significantly affected by way of modeling this region. For this reason, it can be concluded that the deviation of theoretical and experiment results may be due to lack of knowledge about the interfacial zone and its morphology and mechanical characterization.

**Table 2**

Comparison of Elastic modulus calculated by theoretical, experimental, and FE models ( $Wt=3\%$  and  $D_p=25nm$ ).

	Kerner Model	Paul Model	Experiment [25]	FE
$\frac{E_c}{E_m}$	1.114445	0.989353	0.683067	0.673146

## 4 CONCLUSIONS

A comprehensive 3D finite element simulation was implemented to investigate the mechanical and thermal behavior of a polymer matrix nanocomposite reinforced by MMT nanoparticles. From the current study, some conclusion remarks can be obtained as follows:

- The Young's and shear modulus increase by increasing weight fraction of MMT nanoparticles.
- Young's modulus of the nano-reinforced polymer composite increases with decrease in the nanoparticle diameter.

- Nanoparticles carry well stresses induced by loading.
- Adding nanoparticles causes the heat expansion coefficient to decrease while this causes the heat stability of the nano-reinforced polymer composite to increase.
- Increment of weight fraction of MMT nanoparticle increases the heat expansion coefficient of the nano-reinforced polymer composite.
- Heat transfer coefficient of the matrix decreases by adding MMT nanoparticle which this causes the nano-reinforced polymer composite is being an excellent insulation.
- Heat expansion coefficient of the nano-reinforced polymer composite decreases with increase in weight fraction of MMT nanoparticle.
- The modeling and results derivation procedure considered in this paper can be a very effectual tool to analyze reinforced polymer composites with particles.

## REFERENCES

- [1] Fomes T., Paul D., 2003, Modeling properties of nylon 6/clay nanocomposites using composite theories, *Polymer* **44**(17): 4993-5013.
- [2] Karamane M., Raihane M., Tasdelen M.A., Uyar T., Lahcini M., Ilsouk M., 2017, Preparation of fluorinated methacrylate/clay nanocomposite via in-situ polymerization: Characterization, structure, and properties, *Journal of Polymer Science Part A: Polymer Chemistry* **55**(3): 411-418.
- [3] Mahmood W.A.K., Azarian M.H., Fathilah W., Kwok E., 2017, Nanoencapsulation of montmorillonite clay within poly (ethylene glycol) nanobeads by electrospraying, *Journal of Applied Polymer Science* **134**(28): 45048.
- [4] Paliwal B., Lawrimore W.B., Chandler M.Q., Horstemeyer M.F., 2017, Nanomechanical modeling of interfaces of polyvinyl alcohol (PVA)/clay nanocomposite, *Philosophical Magazine* **97**(15): 1179-1208.
- [5] Zeng Q., Yu A., Lu G., 2008, Multiscale modeling and simulation of polymer nanocomposites, *Progress in Polymer Science* **33**(2): 191-269.
- [6] Zeng Q.H., Yu A.B., Lu G.Q., Paul D.R., 2005, Clay-based polymer nanocomposites: research and commercial development, *Journal of Nanoscience and Nanotechnology* **5**(10): 1574-1592.
- [7] Raja S.N., Olson A.C., Limaye A., Thorkelsson K., Luong A., Lin L., 2015, Influence of three-dimensional nanoparticle branching on the Young's modulus of nanocomposites: Effect of interface orientation, *Proceedings of the National Academy of Sciences* **112**(21): 6533-6538.
- [8] Wang Z., Lv Q., Chen S., Li C., Sun S., Hu S., 2016, Effect of interfacial bonding on interphase properties in SiO<sub>2</sub>/epoxy nanocomposite: A molecular dynamics simulation study, *ACS Applied Materials & Interfaces* **8**(11): 7499-7508.
- [9] Han Y., Elliott J., 2007, Molecular dynamics simulations of the elastic properties of polymer/carbon nanotube composites, *Computational Materials Science* **39**(2): 315-323.
- [10] Yang S., Yu S., Kyoung W., Han D-S., Cho M., 2012, Multiscale modeling of size-dependent elastic properties of carbon nanotube/polymer nanocomposites with interfacial imperfections, *Polymer* **53**(2):623-633.
- [11] Zhu H., 1996, Sintering processes of two nanoparticles: a study by molecular dynamics simulations, *Philosophical Magazine Letters* **73**(1): 27-33.
- [12] Smith J.S., Bedrov D., Smith G.D., 2003, A molecular dynamics simulation study of nanoparticle interactions in a model polymer-nanoparticle composite, *Composites Science and Technology* **63**(11): 1599-1605.
- [13] Naicker P.K., Cummings P.T., Zhang H., Banfield J.F., 2005, Characterization of titanium dioxide nanoparticles using molecular dynamics simulations, *The Journal of Physical Chemistry B* **109**(32): 15243-15249.
- [14] Hooper J.B., Schweizer K.S., 2006, Theory of phase separation in polymer nanocomposites, *Macromolecules* **39**(15): 5133-5142.
- [15] Ghosh A., Mandal P., Karmakar S., Ghosh A., 2013, Analytical theory and stability analysis of an elongated nanoscale object under external torque, *Physical Chemistry Chemical Physics* **15**(26): 10817-10823.
- [16] Valavala P., Odegard G., 2005, Modeling techniques for determination of mechanical properties of polymer nanocomposites, *Reviews on Advanced Materials Science* **9**: 34-44.
- [17] Yu S., Yang S., Cho M., 2009, Multi-scale modeling of cross-linked epoxy nanocomposites, *Polymer* **50**(3): 945-952.
- [18] Sheng N., Boyce M.C., Parks D.M., Rutledge G., Abes J., Cohen R., 2004, Multiscale micromechanical modeling of polymer/clay nanocomposites and the effective clay particle, *Polymer* **45**(2): 487-506.
- [19] Spanos P., Kotsos A., 2008, A multiscale Monte Carlo finite element method for determining mechanical properties of polymer nanocomposites, *Probabilistic Engineering Mechanics* **23**(4): 456-470.
- [20] Buryachenko V., Roy A., Lafdi K., Anderson K.L., Chellapilla S., 2005, Multi-scale mechanics of nanocomposites including interface: experimental and numerical investigation, *Composites Science and Technology* **65**(15): 2435-2465.
- [21] Mohammadpour E., Awang M., Kakooei S., Akil H.M., 2014, Modeling the tensile stress-strain response of carbon nanotube/polypropylene nanocomposites using nonlinear representative volume element, *Materials & Design* **58**: 36-42.

- [22] Shahzamanian M., Tadeipalli T., Rajendran A., Hodo W.D., Mohan R., Valisetty R., 2014, Representative volume element based modeling of cementitious materials, *Journal of Engineering Materials and Technology* **136**(1): 011007.
- [23] Ali D., Sen S., 2016, Finite element analysis of the effect of boron nitride nanotubes in beta tricalcium phosphate and hydroxyapatite elastic modulus using the RVE model, *Composites Part B: Engineering* **90**: 336-340.
- [24] Bravo-Castillero J., Rodrigues-Ramos R., Houari M., Otero J., 2009, Homogenization and effective properties of periodic thermo magneto electro elastic composites, *Journal of Materials and Structures* **4**(5): 819-836.
- [25] Lezgy-Nazargah M., Eskandari-Nadaf H., 2018, Effective coupled thermo-electro-mechanical properties of piezoelectric structural fiber composites: A micromechanical approach, *Journal of Intelligent Material Systems and Structures* **29**(4): 496-513.
- [26] Lezgy-Nazargah M., 2015, A micromechanics model for effective coupled thermo-electro-elastic properties of Macro Fiber Composites, *Journal of Mechanics* **31**(2):183-199.
- [27] Huang J., Uhrig M., Weber U., Schmauder S., 2015, Numerical simulation of mechanical properties of nano particle modified polyamide 6 via RVE modeling, *Journal of Materials Science and Chemical Engineering* **3**(01): 95-102.
- [28] Yas M.H., Karami Khorramabadi M., 2017, Preparation with modeling and theoretical predictions of mechanical properties of functionally graded polyethylene/clay nanocomposites, *Journal of Theoretical and Applied Mechanics* **55**(2): 583-593.
- [29] Shojaie M., Golestanian H., 2011, Effects of interface characteristics on mechanical properties of carbon nanotube reinforced polymer composites, *Materials Science and Technology* **27**(5): 916-922.
- [30] Holland J.H., 1992, *Adaptation in Natural and Artificial Systems: An Introductory Analysis with Applications to Biology, Control, and Artificial Intelligence*, MIT Press.
- [31] Bashorov M., Kozlov G., Zaikov G., Mikitaev A., 2009, Polymers as natural nanocomposites, *The Comparative Analysis of Reinforcement Mechanisms* **3**(3): 183-185.
- [32] Zare Y., Rhee K.Y., Hui D., 2017, Influences of nanoparticles aggregation/agglomeration on the interfacial/interphase and tensile properties of nanocomposites, *Composites Part B: Engineering* **122**:41-46.
- [33] Paul B., 1959, *Prediction of Elastic Constants of Multi-Phase Materials*, Brown University Providence.